1.1

INVESTIGATING THE CAUSES OF THE RESPONSE OF THE THERMOHALINE CIRCULATION TO PAST AND FUTURE CLIMATE CHANGES

R. J. Stouffer[1], J. Yin[2*], J. M. Gregory[3,4], K. W. Dixon[1], M. J. Spelman[1], W. Hurlin[1], A. J. Weaver[5], M. Eby[5], G. M. Flato[6], H. Hasumi[7], A. Hu[8], J. H. Jungclaus[9], I. V. Kamenkovich[10], A. Levermann[11], M. Montoya[12], S. Murakami[13], S. Nawrath[11], A. Oka[7], W. R. Peltier[14], D. Y. Robitaille[6], A. Sokolov[15], G. Vettoretti[14], S. L. Weber[16]

1. Geophysical Fluid Dynamics Laboratory/NOAA, Princeton, USA
2. Program in Atmospheric & Oceanic Sciences, Princeton University, USA
3. Department of Meteorology, University of Reading, Reading, UK
4. Hadley Centre for Climate Prediction and Research, Met Office, Exeter, UK
5. School of Earth and Ocean Sciences, University of Victoria, Canada
6. Canadian Centre for Climate Modelling and Analysis, Victoria, Canada
7. Center for Climate System Research, University of Tokyo, Japan
8. National Center for Atmospheric Research, Boulder, USA
9. Max-Planck-Institute for Meteorology, Hamburg, Germany
10. University of Washington, Seattle, USA
11. Potsdam Institute for Climate Impact Research, Germany
12. Department of Astrophysics and Atmospheric Sciences, Universidad Complutense, Madrid, Spain
13. Meteorological Research Institute, Japan
14. Department of Physics, University of Toronto, Canada
15. Massachussetts Institute of Technology, Cambridge, USA
16. Royal Netherlands Meteorological Institute, The Netherlands

1. Introduction

The importance of the Atlantic thermohaline circulation (THC) to climate and climate change stems from its two unique properties: its large northward heat transport and nonlinear dynamical behavior. Here we define the THC as the part of the ocean circulation which involves warm, saline surface water flowing northward and the cold, dense water flowing southward at depth in the Atlantic Basin (Wunsch, 2002). This warm, saline surface water flows into high latitudes of the Northern Hemisphere where it is cooled and sinks to depth. These waters then flow southward at depth through the Atlantic Ocean, mainly as a deep western boundary current, until they reach the Southern Ocean where they mix with the rest of the world ocean waters.

Some past abrupt climate changes are considered to have resulted from rapid reorganizations of the THC (Boyle and Keigwin, 1987; Duplessy *et al.*, 1988; Broecker, 1997; Clark *et al.*, 2002). Modeling studies indicate that the THC is potentially sensitive to changes in surface buoyancy fluxes induced by anthropogenic climate change (Dixon *et al.*, 1999; Mikolajewicz and Voss, 2000; Cubasch *et al.*, 2001; Gregory *et al.*, 2005) and some model simulations have suggested that large changes of the THC are possible in the future (Manabe and Stouffer, 1995; Stocker and Schmittner, 1997). Severe concerns about the future evolution of this critical system have resulted in detailed investigations of the dynamical behavior of the THC and THC-induced climate changes. Although much work has been done (Manabe and Stouffer, 1988, 1995, 1999; Stocker and Wright, 1991; Rahmstorf, 1995; Schiller *et al.*, 1997; Dixon *et al.*, 1999; Vellinga and Wood, 2002; Gregory *et al.*, 2003), the previous research unfortunately points to substantial uncertainties in the model's THC response. For example, the sensitivity of the THC to freshwater addition, the magnitude of the THC-induced cooling, the cooling region, the reversibility of the THC after its collapse etc., are all highly model-dependent. The disagreement among model simulations is a clear indication of the complexity of the THC system. It also reflects limitations in current understanding of how the large-scale climate system operates.

For simulated climate change, all the relevant data are in principle available for analysis and understanding of the model results, yet the reasons for the differences among the models are largely unknown and have not been studied systematically. To address this deficiency and hence reduce the uncertainties in modeling the dynamical behavior of the THC and THC-induced climate change, two sets of coordinated THC experiments were set up as an activity of the Coupled Model Intercomparison Project (CMIP) of the

* *Corresponding author address*:
Jianjun Yin, Program in Amospheric & Oceanic Sciences, Princeton University, Princeton, NJ 08544;
e-mail: Jianjun.Yin@noaa.gov

WMO/WCRP/CLIVAR Working Group on Coupled Models (WGCM, www-pcmdi.llnl.gov/cmip/coord_expt.html). One set of coordinated experiments (so-called "water-hosing" – see below) is also an activity of the Paleo-Modeling Intercomparison Project (PMIP), also part of the WCRP (World Climate Research Programme).

The coordinated experiments comprise simulations of a common design being undertaken at institutions worldwide using their own climate models, either coupled atmosphere-ocean general circulation models (AOGCMs) or Earth system models of intermediate complexity (EMICs). AOGCMs are the main tools used for climate prediction, but require large computing resources, so EMICs are also widely used to study past or future climate changes. Table 1 lists the participating institutions and models used in this study.

Model	Institute
CCC_CGCM2	Canadian Centre for Climate Modelling & Analysis, Canada
CLIMBER_2	Potsdam Institute for Climate Impact Research, Germany
CLIMBER_3α	Potsdam Institute for Climate Impact Research, Germany
ECBilt/CLIO	Royal Netherlands Meteorological Institute, The Netherlands
ECHAM5/ MPI-OM	Max-Planck Institute for Meteorology, Germany
GFDL_CM2.1	Geophysical Fluid Dynamics Laboratory, USA
GFDL_R30	Geophysical Fluid Dynamics Laboratory, USA
HadCM3	Hadley Centre for Climate Prediction & Research, UK
MIROC3.2	University of Tokyo Japan
MIT_UWash	Massachusetts Institute of Technology & University of Washington, USA
MRI_CGCM2. 3	Meteorological Research Institute, Japan
NCAR_CCSM 2.0	National Center for Atmospheric Research, USA
UToronto	University of Toronto, Canada
UVic	University of Victoria, Canada

Table 1. Participating models

The purpose of the coordinated experiments is to assess the differences in model responses and investigate the reasons for those differences. By combining representative model simulations in a multi-model ensemble, the robustness of a particular simulation feature can be evaluated. The set of so-called "partially coupled" experiments, allows the role of the surface fluxes in the weakening of the THC when greenhouse gases increase to be investigated (Gregory *et al.*, 2005). In the second set of experiments, the so-called water-hosing simulations, the response of the THC to a specified external source of freshwater and the resulting climate change are studied. This water-hosing experimental design is highly idealized. Its results have implications not only for future climate changes, but also to help understand past climate changes seen in the paleo-record. The implication for increasing understanding of past climate changes encouraged the Paleo-Modeling Intercomparison Project (PMIP) to co-support this second experiment along with CMIP.

2. Design of the Water-Hosing Experiments

The water-hosing experiments studies the sensitivity of the THC to an external source of freshwater. In a perturbation experiment, an additional freshwater flux of 0.1 Sv is applied for 100 years to the northern North Atlantic Ocean. The external water flux is then switched off after model year 100 and the integration continues, in order to investigate whether or not the THC recovers its initial strength and the rate of the recovery. A control integration, with no external water flux forcing, runs in parallel to the perturbation integration. The size of the forcing ("hosing") freshwater flux, which is approximately equal to the runoff of the Amazon River, was chosen to be of the order of magnitude predicted for a large CO_2–induced climate change. For instance, at $4xCO_2$ in HadCM3 (experiment 2PC of Wood *et al.*, 1999), the increase in water flux from precipitation, evaporation and river runoff into the Arctic and Atlantic Oceans north of 45°N is 0.14 Sv. Similar freshwater flux changes were simulated for the late 21st century in a version of GFDL's R15 model (Fig. 3 of Dixon *et al.*, 1999). These fluxes are thought to be the dominant terms in the water budget over the next 100 years. The Greenland ice sheet might add about half as much; in the most extreme scenarios considered in the IPCC Third Assessment Report (Church *et al.*, 2001), melting of the ice sheet contributes about 6 mm/yr to global average sea level rise, equivalent to 0.07 Sv. Melting of perennial Arctic sea ice gives a term an order of magnitude smaller; a volume of 2×10^{13} m^3 melting in 50 years yields a flux of 0.01 Sv.

The hosing flux is applied uniformly over the Atlantic between 50° and 70°N. This is obviously an idealization, and there will be some sensitivity to the region chosen (Rahmstorf, 1996; Gregory *et al.*, 2003). A broad area is chosen so as to ensure the model-to-model variations in the location of deep convection are likely to be situated under the region of freshening. It also helps solve limitations found in many ocean general circulation models to handle large local water fluxes. These limitations are due to the assumptions used in the model construction (for example, the so-called rigid lid used to filter the fast waves observed in the ocean) and in the numerical algorithms used to compute advection of water properties. Ocean models are now being constructed that do not suffer from these issues (see Griffies 2004 as one example). However most of the models used here have these limitations

and therefore a large area was chosen for the water hosing forcing in an attempt to minimize the effect of the numerical issues on the results presented below.

After obtaining the results from the standard water-hosing experiment, some groups performed a second water-hosing experiment. In this experiment, the design is the same as described above except that the rate is 10 times larger, 1.0 Sv, approximately equal to the total global river runoff. This rate is sufficient to shut down the THC in some models over 30 years or less. A water flux as large as 1.0 Sv is extremely unlikely under realistic CO_2 scenarios, however this flux is within the range envisaged for events driven by meltwater release during the last glacial era and the deglaciation (Clarke *et al.*, 2003), though not for periods as long as a century. This rate would add about 9 m of globally averaged sea level over a 100 year period. In addition, similar sea level rises have been caused by the massive iceberg discharges from the Laurentide Ice Sheet during the Heinrich events (Calov *et al.*, 2002; Chappell, 2002). Over a 1000 year period, these discharges could induce a freshwater flux on the order of 0.1 Sv.

3. Results

3.1. 0.1 Sv Water-Hosing Experiment

In the present study, we mainly summarize the simulations in terms of the mean of the model as an ensemble and focus on selected variables. To construct the geographical distribution of the ensemble mean, the models' results are first interpolated to a common 1°x1° grid. The mean value at each common point is then calculated and plotted using all available model simulations.

3.1.1. The THC Response

The sensitivity of the THC to external freshwater forcing varies among different climate models (Bryan, 1986; Schiller *et al.*, 1997; Manabe and Stouffer, 1999). In response to freshwater perturbation, the reduction of the THC intensity is proportional to both the magnitude and duration of the perturbation (Rind *et al.*, 2001). Due to the slow adjustment of the deep ocean, the integrations are transient and not equilibrium responses (Stouffer, 2004). Here we define the THC intensity as the maximum meridional overturning streamfunction value in the North Atlantic excluding the surface wind-driven overturning circulation. The THC intensity varies greatly among the control runs of the participating models (Fig. 1). There are large differences in terms of the mean intensity and in the amplitude and period of its multi-decadal variations. The model results can be classified into three groups according to the characteristics of the THC in the control runs. The first group includes the GFDL_CM2.1, GFDL_R30, HadCM3, ECBILT_CLIO and UToronto models. The THC in these models is vigorous and presents pronounced multi-decadal variations. The second group includes CCC_CGCM2, ECHAM5/MPI-OM, MIROC3.2, MRI_CGCM2.3 and NCAR_CCSM2.0. In these models, the THC is relatively weak and the amplitude of its multi-decadal variations is small. CLIMBER, MIT_UWash and UVic belong to the third group, in which the THC has little variation. The models in this last group do not incorporate an atmospheric component which resolves synoptic variability. Therefore, they do not generate enough "noise" to excite multi-decadal oscillations of the THC. The reasons why the decadal time scale variability between the first two groups differs so much, and why the mean THC intensity varies widely among all the models, are not clear. Possible mechanisms for these differences have been suggested in previous research work (Weaver *et al.*, 1991; Delworth *et al.*, 1993; Timmermann *et al.*, 1998) and is the possible subject for future investigations.

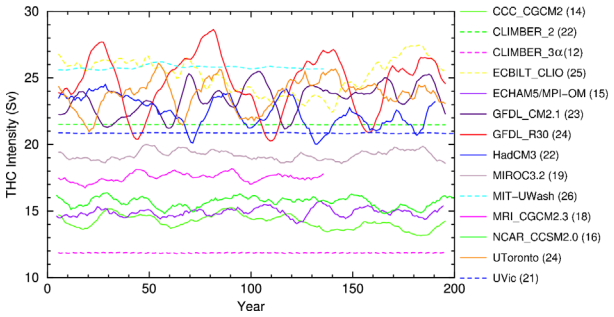

Fig. 1. Time series of the THC intensity (Sv) in the control runs. A 10-year running mean was performed on the curves to reduce the high-frequency fluctuations of the THC. Solid curves for AOGCMs and dashed curves for EMICs. The numbers after the model names indicate the long-term mean of the THC intensity.

The THC intensity anomalies (Fig. 2) in the 0.1 Sv water-hosing experiment indicate that the THC weakens in all the models in response to the freshwater input at the ocean surface in high latitudes of the North Atlantic . A 10-year running mean was performed on the curves to reduce the high-frequency fluctuations of the THC intensity caused by the wind stress variations. Starting from initial conditions, the curves diverge with time as the freshwater is added, indicating differing freshwater sensitivity of the THC among models. The reduction of the THC intensity at the 100th year ranges from 1.3 to 9.7 Sv (Fig. 2a) or from 9% to 62% relative to the control (Fig. 2b). The black curve gives the multi-model ensemble mean of 5.6 Sv, equivalent to a 30% weakening of the THC after 100 years of freshwater input. The difference in the THC sensitivity to freshwater input among models is an important issue as it affects all aspects of the climate response (shown later). The numerical schemes, grid resolution, the control climate THC simulation, the location of deep convection, the ocean currents, and the salinity distribution might all be factors in determining this difference. We find no significant correlation between the absolute weakening of the THC and the THC strength in the control runs. For example, the THC intensity simulated by GFDL_R30

and CCC_CGCM2 in the control runs are 24 and 14 Sv respectively, representing a strong and a weak THC flow. However, both models simulate a similar 9~10 Sv absolute reduction of the THC intensity by the end of the freshwater input period.

Due to the slow adjustment of the deep ocean, the THC doesn't reach equilibrium with the external freshwater forcing during the period of freshwater input. Generally, the THC decreases more rapidly within the first several decades of the 0.1 Sv water-hosing experiment and the rate of decrease lessens thereafter. In addition, not all models simulate the weakest THC at the end of the freshwater perturbation. The THC intensity in the HadCM3, MIT_UWash and UToronto models all reach their minimum before the 100th year of the simulation and shows signs of re-intensification even under the continuing freshwater forcing. These re-intensifications seem related to a switch of the major deep convection sites to locations north of the hosing area in these models. This shift is likely a result of the experimental design. If the hosing area extended further north, it is likely that this shift would not occur. Finally, it needs to be noted that the freshwater perturbation of 0.1 Sv for 100 years is insufficient to shut down the THC in any of the models presented here.

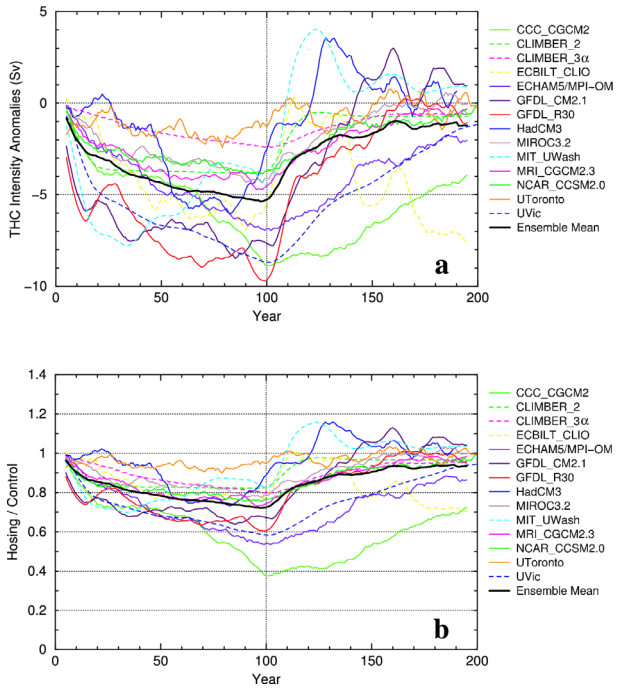

Fig. 2. Time series of the THC intensity anomalies in the 0.1 Sv water-hosing experiments. (a) The absolute value of the anomalies; (b) The relative anomalies compared with the long-term mean of the THC intensity in the control experiments. Solid curves for AOGCMs and dashed curves for EMICs.

After the termination of the freshwater perturbation, the THC starts recovering towards its control strength. Thus, no critical point like Stommel's saddle-node bifurcation (Stommel, 1961; Rahmstorf, 1995) beyond which the THC collapses completely has been passed in these model simulations. The time scale of the THC recovery varies greatly among the models. Two models with the largest fractional decrease, CCC_CGCM2 and ECHAM5/MPI-OM (Fig. 2b), have the longest re-intensification time, whereas the THC in other models recovers to a value similar to the control within several decades after the freshwater perturbation ends. The THC in CCC_CGCM2 and ECHAM5/MPI-OM is still well below their respective control intensities at the 200th year. In the GFDL_CM2.1, HadCM3 and MIT_UWash models, it appears that the THC overshoots the control run during the recovery phase, but eventually comes back to its control value. It seems that the deep convection activities at the original sites in these models resume quickly after the termination of the freshwater perturbation, while those north of the hosing region do not switch off immediately.

3.1.2. Surface Air Temperature

Both the magnitude and geographical distribution of the THC-induced surface air temperature (SAT) change, particularly the cooling over the northern North Atlantic varies greatly among the model simulations. As shown by Fig. 3, four AOGCMs (CCC_CGCM2, ECHAM5/MPI-OM, GFDL_CM2.1 and GFDL_R30) and two EMICs (ECBILT_CLIO and UVic) simulate significant cooling with a pronounced center south of Greenland in response to 0.1 Sv freshwater perturbation. In contrast, the other five AOGCMs (HadCM3, MIROC3.2, MRI_CGCM2.3, NCAR_CCSM2.0 and UToronto) and one EMIC (CLIMBER_3α) obtain very weak temperature decrease over the northern North Atlantic without any notable cooling center.

An interesting feature in Fig. 3 is the warming over the Barents and Nordic Seas. It appears in four AOGCMs (GFDL_R30, HadCM3, MIROC3.2 and UToronto) and one EMIC (ECBILT_CLIO). The warming in this region is as large as 10°C in the MIROC3.2 and UToronto results, and 5°C in the HadCM3. It can be larger in magnitude than the cooling south of Greenland. The warming is caused by the northward shift of oceanic deep convection, the resulting increase in the northward heat transport in the high latitudes of the North Atlantic and then amplified by a sea ice feedback. The perturbation freshwater flux weakens the deep convection in the 50°~70°N belt. It is possible for the sinking to take place further north in the Barents Sea, where no perturbation freshwater flux is directly imposed and conditions can be favorable for water mass formation to occur. As a result, in some models the sinking moves north into the Barrents Sea. The ECBILT_CLIO, GFDL_R30, HadCM3 and

MIROC3.2 models indeed show a positive SSS anomaly in the Barents Sea associated with the enhanced deep water formation there, while the UToronto model shows positive anomalies in the Greenland-Iceland-Norwegian (GIN) Seas and south of Greenland.

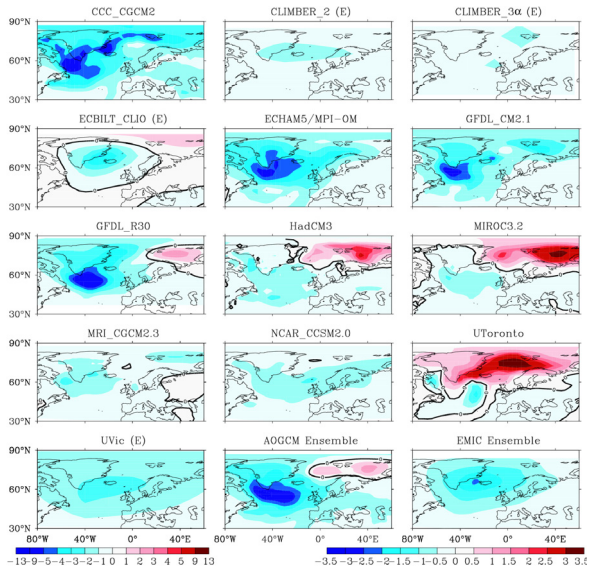

Fig. 3. The surface air temperature anomalies (Y81~100) simulated by different models in the 0.1 Sv water-hosing experiment. The difference is constructed by subtracting Y81~100 of the hosing integration from Y1~100 of the control. "E" indicates that the model is an EMIC. The last two ensemble panels use a different scale.

The increased convection brings relatively warmer seawater from the ocean interior to the surface. This heating from below reduces the sea ice thickness and pushes back the sea ice boundary. The lower atmosphere no longer overlies sea ice which insulates the atmosphere from the ocean. The heat from the ocean then warms the overlying atmosphere, leading to the large SAT changes seen in Fig. 3 in some models. For the models in which the simulated sea ice in the Barents and Nordic Seas is thick, this warming can be quite large.

The response in the Southern Hemisphere to the slowdown of the THC is much smaller than seen in the Northern Hemisphere (not shown). Generally there is a small warming in the Southern Hemisphere. As the THC weakens, the northward heat transport is reduced, keeping more heat in the Southern Hemisphere. This additional heat leads to the small SAT warming found there.

Much of the SAT change essentially stems from the change of northward heat transport in the Atlantic as noted above. The heat transport in the Atlantic is uniformly northward, differing from the simulation in the Pacific Ocean where the heat transport is poleward. Among the models analyzed here, the maximum northward heat transport at about 20°N in the North Atlantic Ocean ranges from 0.7 to 1.1 PW (1 PW=10^{15} Watts). This is weaker than the observed estimate of about 1.3 PW, but within the uncertainty range (Ganachaud and Wunsch, 2000). After the slowdown of the THC, the northward heat transport in the Atlantic decreases. The multi-model ensemble mean gives a maximum decrease about 0.13 PW around 20°N.

3.1.3. Ocean Temperature and Salinity

The multi-model ensemble change of SST (Fig. 4a) after the slowdown of the THC bears similar pattern with that of the surface air temperature. The SST decrease up to 3°C south of Greenland extends the sea ice coverage in this region. The slight SST increase in the Barents Sea corresponds to the SAT warming. The slight warming of the SST in the South Atlantic, induced by the slowdown of the THC, spreads throughout the Southern Ocean via the Antarctic Circumpolar Current (ACC). The fulcrum of the SST changes is the equatorial Atlantic. Besides the thermal effect on the atmosphere, the decrease of the SST over the northern North Atlantic also provides the so-called temperature advection feedback to stabilize the THC by increasing the surface seawater density. But this effect is secondary in comparison with the density decrease induced by the high-latitude freshening due to the hosing.

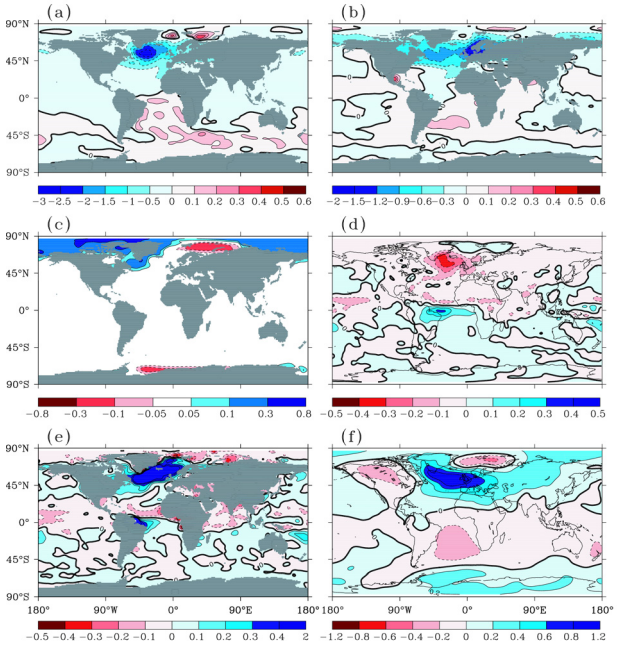

Fig. 4. Geographical distribution of the ensemble mean anomalies in the 0.1 Sv experiment. Y81~100. (a) SST; °C (b) SSS; psu (c) Sea ice thickness; m (d) Precipitation; mm/day (e) Net freshwater flux into the ocean; mm/day (f) Sea level pressure. mb

The decrease in SSS over the northern North Atlantic is a direct result of the additional freshwater input and the response to the weakening of the THC. The multi-model ensemble mean shows that the maximum freshening occurs in the 50°~70°N latitudes with SSS decrease about 1.2 psu. However, different models simulate distinctly different geographical distribution of the SSS anomalies. For example, the maximum freshening can occur at the eastern, middle or western part of 50°~70°N latitudes of the North Atlantic. Some models obtain a positive SSS anomaly around the Barents Sea while some others simulate a negative anomaly there. The differences in the SSS response could result from many factors such as the location of the deep convection sites or the exact details of the time mean oceanic currents. Generally, the North Atlantic surface water becomes fresher and the South Atlantic becomes saltier during the slowdown of the THC. The salinity increase in Gulf of Mexico and the Caribbean Sea is a consequence of the change of evaporation and precipitation there. Sedimentological data have confirmed that the SSS in the Caribbean Sea indeed has an anti-phase relationship with North Atlantic Deep Water formation during the last glacial cycle (Schmidt *et al*., 2004).

Unlike SST that can thermally feedback on the overlying atmosphere, SSS plays its major role in the dynamics of the THC and other oceanic circulations. The decrease in salinity in northern North Atlantic and the increase in the tropical-subtropical western North Atlantic create a sharp north-south salinity gradient around 40°N. The northward salinity flux across 40°N increases subsequently accompanying with the ocean horizontal mixing process and gyre circulation. This increase in northward salinity flux in the upper ocean prevents the run-away salinity decrease in the northern North Atlantic induced by the positive salinity-advection feedback associated with the THC (Stommel, 1961).

The large value of salinity decrease and small value of model deviation imply that the Labrador Sea and surrounding oceans are the most susceptible regions to the freshwater perturbation induced either by the increase of P-E or by the melting of nearby ice sheet (Wood *et al*., 1999; Weaver *et al*., 2004; Cheng and Rhines, 2004). The lack of the direct supply of high-salinity seawater makes the deep convection and deep water formation in these regions easier to shut down.

3.1.4. Sea Ice

Sea ice is more extensive and its thickness increases in the Labrador Sea after the slowdown of the THC (Fig. 4c). These changes provide positive feedbacks to enhance the surface air temperature anomalies induced by the reduction of the northward heat transport in the Atlantic. However, due to the northward shift of the deep convection sites and the enhancement of the deep convection, the sea ice retreats and its thickness reduces in the Barents and GIN Seas in the multi-model ensemble. At the southern end of the Atlantic, the sea ice mass also reduces due to the enhancement of the deep convection in the Weddell Sea. As discussed earlier, more heat is transported from the interior ocean to the surface to melt the sea ice.

3.1.5. Precipitation

Previous research on the climate impacts of a slowdown/shutdown of the THC has focused on the surface air temperature change over the high-latitude region. Recently, attention has been given to the tropical-subtropical Atlantic emphasizing the impact of the THC on the hydrological cycle there (Chiang and Koutavas, 2004). The importance of the hydrological cycle over the tropical Atlantic lies in its direct influence on the Amazon's biotic system, the Sahel drought and the low-latitude SSS. The latter helps regulate the intensity of the THC through northward salinity advection, providing complex feedbacks on the dynamical behavior of the THC (Vellinga and Wood, 2002).

After the slowdown of the THC, a dipole pattern in precipitation appears with positive anomalies over the equatorial Atlantic and the Amazon and negative anomalies over the tropical North Atlantic (Fig. 4d). The positive anomaly band spans the entire Atlantic just south of the equator, from the Amazon to central Africa with the center close to northeastern Brazil. Given the annual mean position of the Atlantic ITCZ is in the Northern Hemisphere, this dipole pattern is a signal of the southward shift of the ITCZ and Hadley circulation. The signal is much more significant in the 1.0 Sv water-hosing experiment after the shutdown of the THC.

The shift of the Atlantic ITCZ is mainly attributable to the interhemisphere seesaw pattern of the temperature change over the Atlantic. Notice that there is also a precipitation change dipole over the equatorial Pacific. Given the large total precipitation there, the statistical significance of this dipole remains unclear and is the subject for future investigations.

Besides the low-latitude Atlantic, another region in Fig. 4d where the precipitation also undergoes significant change is the North Atlantic along the mid-latitude storm track. This decrease is closely related to the temperature decrease over the northern North Atlantic and the resulting weakening of the Icelandic Low.

3.1.6. Net Freshwater Flux over the Ocean Surface

The regions where deep convection and deep water formation take place are likely to be the regions where the THC is the most sensitivity to freshwater perturbations. However, the THC can feel any change of the net freshwater flux along its "catchment" region. Essentially, the "catchment" region is the upper route of the THC including the tropical-subtropical Atlantic. Manabe and Stouffer (1995) found freshwater flux

anomalies away from the oceanic convection sites are less effective in causing changes in the THC, than the same anomalies over the oceanic convection sites. Therefore, the evolution of the THC intensity actually is a result of the complex interplay of the net freshwater flux changes in the "catchment" region. It has been shown in the preceding section that the freshwater addition over the northern North Atlantic alters the hydrological cycle in the low-latitude Atlantic. The subsequent freshwater flux anomalies over the tropical-subtropical North Atlantic can provide feedbacks on the freshening over the high-latitude North Atlantic and the intensity of the THC. The net freshwater flux (precipitation plus runoff minus evaporation) anomalies in the 0.1 Sv water-hosing experiment (Fig. 4e) shows a large positive area over the northern North Atlantic resulting from the perturbation freshwater input. Over the low-latitude Atlantic, there is a dipole pattern. We expect that the change of evaporation over the low-latitude Atlantic is relatively small when compared to the local precipitation changes. It seems therefore that the precipitations are the main contributor to the net freshwater flux anomalies. Both the local freshwater fluxes from the atmosphere and the runoff of Amazon River increase after the southward shift of the Atlantic ITCZ. The negative anomalies over the tropical North Atlantic tend to enhance the SSS over low-latitude Atlantic and are then advected northward, offsetting some of the freshening over the high-latitude of the North Atlantic (Lohmann, 2003).

3.2. 1.0 Sv Water-Hosing Experiments

A subset of models performed this second perturbation integration. Since the imposed 1.0 Sv freshwater forcing is an order of magnitude larger, the climate changes are expected to be much larger than those in the 0.1 Sv hosing case.

In response to the 1.0 Sv freshwater input, the THC collapses to a near shutdown condition within 50 years of the start of the freshwater perturbation (Fig. 5). Four models (GFDL_CM2.1, MIT_UWash, NCAR_CCSM2.0 and UToronto) show a rapid re-intensification of the THC once the freshwater is eliminated at the 100th year. Although the integration time is too short for a full response, the shutdown of the THC in the HadCM3 is also likely a reversible process. In contrast, the THC remains inactive in the GFDL_R30 and UVic models even after the termination of the freshwater perturbation, indicating that the THC may have changed states in these two models.

The AOGCM ensemble mean of the SAT anomalies after the shutdown of the THC shows a large cooling in the North Atlantic (Fig. 6q). The maximum cooling of up to 12°C occurs between Scotland and Iceland, while the western and northern Europe becomes 4°~10°C colder. The temperature over the tropical North Atlantic also decreases about 2°~3°C. The maximum warming of up to 2.4°C occurs over the South Atlantic along the Africa coast. This warming is induced by the redistribution of the oceanic heat carried by the THC.

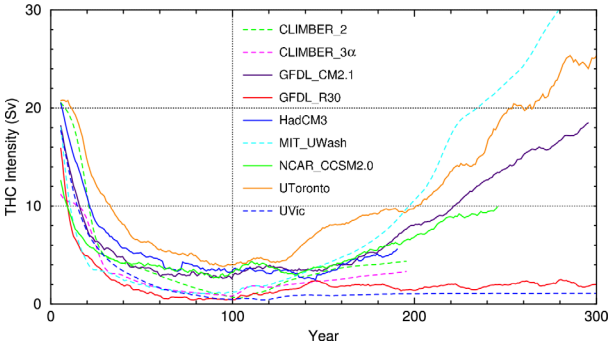

Fig. 5. Time series of the THC intensity evolution in the 1.0 Sv water-hosing experiments.

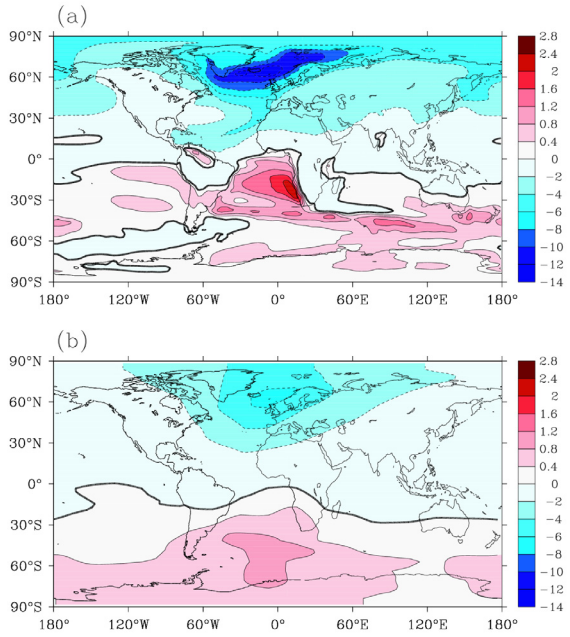

Fig. 6. The SAT anomalies (Y81~100) in the 1.0 Sv experiment. (a) AOGCM ensemble; (b) EMIC ensemble.

On average, the Northern Hemisphere as a whole cools about 2.3°C and the Southern Hemisphere warms about 0.3°C . Consequently, there is a global cooling about 1°C after the shutdown of the THC. The EMICs simulate similiar SAT anomaly patterns as the AOGCMs but with relative smaller magnitude (Fig. 6b). The ensemble EMIC mean cooling of the Northern Hemisphere is about 1.4°C with the maximum up to 7°C in the northern North Atlantic. The warming in the Southern Hemisphere is also smaller in the EMICs than in the AOGCMs.

After the collapse of the THC, the northward heat transport in the Atlantic Ocean is greatly reduced in

most models. This reduction in the northward heat transport leads to the pattern of SAT changes noted above where the Northern Hemisphere cools and the Southern Hemisphere warms. The magnitude of the local SST and SSS decreases in the North Atlantic can be up to 10°C and 10 psu respectively. The maximum decrease in SST and SSS occurs at the eastern North Atlantic. Most of the North Atlantic north of 50°N is covered by sea ice in winter.

4. Discussion and Conclusion

The coordinated experiments conducted by CMIP/PMIP are designed to improve our understanding of the THC response. Through the increased understanding, the uncertainty associated with the THC response should decrease. This paper represents a first attempt to document the model's THC response in these coordinated experiments.

A 0.1 Sv freshwater perturbation over the 50°~70°N of the North Atlantic approximately resembles the projected freshwater flux anomalies over the high latitudes of the North Atlantic induced by global warming a century or more in the future. In response to this freshwater input, the THC gradually weakens by 30% at the 100th year in the multi-model ensemble mean, with a range of results from the individual models. No model presented here simulates a complete THC shutdown during the 100-year 0.1 Sv perturbation.

It is important to remember the experimental design when applying these results to either past or future climates. A caveat that applies to future climates is that the role of the freshwater flux anomalies in the low latitudes of the Atlantic is not taken into account. It has been demonstrated that the freshwater flux anomalies in the tropical-subtropical Atlantic induced by a reduction in the Amazon River flow in the warmer climate can, in some models, compensate the high latitude surface ocean freshening (Latif *et al.*, 2000, Thorpe *et al.*, 2001). A caveat for applying these results to past climates is that the mean state for these experiments is today's climate. In climates where meltwater from melting land ice is important, it is likely that the mean climate was much colder than today.

In contrast to the uniformly large cooling typically simulated after the shutdown of the THC, the SAT anomalies over the northern North Atlantic present more complex patterns after the slowdown of the THC. A SAT dipole, with cooling south of Greenland and warming over the Barents and Nordic Seas, is indicated by the multi-model ensemble change. Although this dipole might be a function of the location of the hosing region, it reveals that in response to a moderate freshwater addition, the northern convection sites have an anti-correlation with the more southern convection sites in the North Atlantic. The SAT changes seen here also have this pattern. Given the rapid freshening recently observed in the Labrador Sea (Dickson *et al.* 2002) and the reconstruction of the 8200BP event, a period where the Labrador Sea deep convection was disrupted (Barber *et al.*, 1999), this SAT change pattern provides important implications for both past and future climate changes. The maximum cooling about 3°C south of Greenland in response to the 0.1 Sv hosing tends to offset the CO_2 induced warming in the future, so that most models simulate little surface temperature change in this area as the GHG increase (Cubasch *et al.*, 2001).

The 1.0 Sv experiment is more relevant to the past abrupt climate changes. In response to 1.0 Sv freshwater perturbation, the THC weakens rapidly and almost disappears in most models. Both the northward heat and salt transports in the Atlantic Ocean reduce dramatically as the THC shuts down in this experiment. Consequently, the Northern Hemisphere cools and the Southern Hemisphere warms relative to the control integration, with the NH cooling being much larger than the SH warming. The simulated SAT change over the North Atlantic is comparable in magnitude to the paleoclimate reconstruction of the SAT change during the past abrupt climate changes such as the Younger Dryas event (Alley, 2000).

Some models show a recovery of the THC after the elimination of the freshwater perturbation whereas others do not. The mechanism for this different dynamical behavior of the THC is not completely understood. Possible reasons could be: (1) some models may not have stable off state of the THC (Gregory *et al.*, 2003, Romanova *et al.*, 2004); (2) the hosing duration is too short; (3) the hosing amount is too small. For the first reason, it has been shown that the effective oceanic vertical diffusivity (Manabe and Stouffer, 1999, Schmittner and Weaver, 2002; Prange *et al.*, 2003), the representation of feedback processes (Vellinga and Wood, 2002, De Vries and Weber, 2005) and the boundary conditions (Ganopolski and Rahmstorf, 2001) are crucial factors to influence the stability of the off mode of the THC. Their different representations result in differing strengths of the nonlinearity of the THC and differing locations of the bifurcation (if it exists). Considering the potential slowdown of the THC during this century, the reversibility/irreversibility of the THC after its shutdown is an important issue for policy-makers.

One of the interesting features of this study is the mixture of AOGCM and EMIC results in the same study. This allows the comparison of the EMIC model responses to the AOGCM responses given a common forcing. The EMICs used in this study can be split into 3 groups. In one group, the atmosphere is greatly simplified; however the other components are similar in complexity (in some cases, even more complex) to those found in the AOGCMs. The CLIMBER_3α, MIT-UWash and UVic models are examples of this group. A second EMIC group is the models where the atmosphere is somewhat simplified and again the ocean is a general circulation model (GCM). ECBILT_CLIO is an example of this group. Finally,

there are EMICs where both the atmosphere and ocean are quite simple. CLIMBER_2 is an example of this last group (Claussen *et al.*, 2002).

Using these groupings, the EMIC's response is compared to the AOGCMs for this particular study where the forcing is applied to the ocean. For the first and second groups where the ocean component is a GCM, the oceanic responses are very similar to the AOGCMs. When the forcing is quite large (1.0 Sv), the atmospheric response seems different. The longitudinal SAT changes have smaller magnitude than those found in the AOGCMs. Also, the southward movement of the ITCZ was not as pronounced or sharp in these EMICs. The response of the last group using simplified atmosphere and ocean components is also quite similar to the AOGCMs. There are some noticeable differences even in the relatively small forcing case (0.1 Sv, see the heat transport changes for example). It is unclear if those changes are statistically or physically significant. In spite of the differences noted above, it is surprising how well the EMIC responses compare to the AOGCM responses. In most of the figures presented here, the EMIC and AOGCM responses are quite similar. This result gives added confidence to the use of EMICs to study other aspects of climate.

Although many robust simulation features have been revealed, there are still clear differences and disagreements among models in simulating the THC, such as its sensitivity to freshwater addition, its multi-decadal variations, and the reversibility after its shutdown. The understanding of these differences needs more detailed analyses in the future and will help further improve the ability to simulate this critical system.

Acknowledgements

We wish to thank T. Delworth, M. Harrison and J. Russell for useful comments which improved earlier versions of this manuscript. We also thank two anonymous reviewers for their reviews, and our respective funding agencies for support.

References

Alley, R. B., 2000: The Younger Dryas cold interval as viewed from central Greenland. *Quaternary Science Reviews*, **19**, 213-226.

Barber, D. C. et al. 1999: Forcing of of the cold events of 8200 years ago by catastrophic drainage of Laurentide lakes. *Nature*, **400**, 344-348.

Boyle, E. A., and L. D. Keigwin, 1987: North Atlantic thermohaline circulation during the past 20,000 years linked to high-latitude surface temperature. *Nature,* **330,** 35-40.

Broecker, W. S., 1997: Thermohaline circulation, the achilles heel of our climate system: Will man-made CO_2 upset the current balance? *Science*, **278**, 1582-1588.

Bryan, F., 1986: High-latitude salinity effects and interhemispheric thermohaline circulations. *Nature*, **323**, 301-304.

Calov, R., A. Ganopolski, V. Petoukhov, M. Claussen, and R. Greve, 2002: Large-scale instabilities of the Laurentide ice sheet simulated in a fully coupled climate-system model, *Geophys. Res. Lett.*, *29(*24), 2216, doi:10.1029/2002GL016078.

Chappell, J., 2002: Sea level changes forced ice breakouts in the Last Glacial cycle: new results from coral terraces, *Quat. Sci. Rev.*, *21*(10), 1229– 1240.

Cheng, W., and P. B. Rhines, 2004: Response of the overturning circulation to high-latitude freshwater perturbations in the North Atlantic. *Climate Dyn.,* **22**, 359-372.

Chiang, J. C. H. and A. Koutavas, 2004: Tropical flip-flop connections. *Nature*, **432**, 684-685.

Church, J. A., et al. 2001: Change in sea level. In: Climate Change 2001: The Scientific Basis. Contribution of Working Group I to the Third Assessment Report of the Intergovernmental Panel on Climate Change [Houghton J.T. et al. (eds.)]. Cambridge University Press, pp. 640-693.

Clark, P. U., N. G. Pisias, T. F. Stocker and A. J. Weaver, 2002: The role of the thermohaline circulation in abrupt climate change. *Nature*, **415**, 863-869.

Clarke, G. K. C., D. W. Leverington, J. T. Teller, A. S. Dyke, 2003: Superlakes, megafloods, and abrupt climate change. *Science*, **301**, 922-923.

Claussen, M., Mysak, L.A., Weaver, A.J., Crucifix, M., Fichefet, T., Loutre, M.-F., Weber, S.L., Alcamo, J., Alexeev, V.A., Berger, A., Calov, R., Ganopolski, A., Goosse, H., Lohman, G., Lunkeit, F, Mokhov, I.I., Petoukhov, V., Stone, P., Wang, Zh., 2002: Earth System Models of Intermediate Complexity: Closing the Gap in the Spectrum of Climate System Models, *Climate Dyn.*, 18, 579-586.

Cubasch U., *et al.* 2001: Projections of future climate change. In: Climate Change 2001: The Scientific Basis. Contribution of Working Group I to the Third Assessment Report of the Intergovernmental Panel on Climate Change [Houghton J.T. et al. (eds.)]. Cambridge University Press, pp. 525-582.

Delworth, T., S. Manabe, and R. J. Stouffer, 1993: Interdacadal oscillation of the thermohaline circulation in a coupled ocean-atmosphere model. *J. Climate,* **6,** 1993-2011.

——, R. J. Stouffer, K. W. Dixon, M. J. Spelman, T. R. Knutson, A. J. Broccoli, P. J. Kushner, and R. T. Wetherald, 2002: Review of simulations of climate variability and change with the GFDL R30 coupled climate model. *Climate Dyn.*, 19(7), 555-574.

Dickson, B., I. Yashayaev, J. Meincke, B. Turrell, S. Dye and J. Holfort, 2002: Rapid freshening of the deep North Atlantic Ocean over the past four decades. *Nature*, 416, 832-837.

Dixon, K. W., T. Delworth, M. Spelman and R. J. Stouffer, 1999: The influence of transient surface fluxes on North Atlantic overturning in a coupled GCM climate change experiment. *Geophy. Res. Lett*, **26**, 2749-2752.

Duplessy, J.-C. *et al.*, 1988: Deepwater source variations during the last climatic cycle and their impact on the global deepwater circulation. *Paleoceanography* **3**, 343_360.

Ganachaud, A. and C. Wunsch, 2000: Improved estimates of global ocean circulation, heat transport and mixing from hydrographic data. *Nature*, **408**, 453–456.

Ganopolski, A., and S. Rahmstorf, 2001: Rapid changes of glacial climate simulated in a coupled climate model. *Nature*, **409**, 153–158.

Gregory, J. M., O. A. Saenko, A. J. Weaver, 2003: The role of the Atlantic freshwater balance in the hysteresis of the meridional overturning circulation. *Climate Dyn.,* **21**, 707-717.

—— *et al.*, 2005: A model intercomparison of changes in the Atlantic thermohaline circulation in response to increasing atmospheric CO_2 concentration. *Geophy. Res. Lett*, 32, L12703,doi:10.1029/2005GL023209.

Griffies, S. M. 2004: Fundamentals of Ocean Climate Models. Princeton, NJ: Princeton University Press, 496 pp.

Hansen, B., and S. Osterhus, 2000: North Atlantic-Nordic Seas exchanges. *Progress in Oceanography*, **45**, 109-208.

Latif, M., E. Roeckner, U. Mikolajewicz, and R. Voss, 2000: Tropical stabilization of the thermohaline circulation in a greenhouse warming simulation. *J. Climate,* **13**, 1809-1813.

Levermann, A., A Griesel, M. Hofmann, M. Montoya, S. Rahmstorf, 2005: Dynamic sea level changes following changes in the thermohaline circulation. *Climate Dynamics*, **24**, 347-354.

Lohmann, G., 2003: Atmospheric and oceanic freshwater transport during weak Atlantic overturning circulation. *Tellus*, **55A**, 438-449.

Manabe, S., and R. J. Stouffer, 1988: Two Stable Equilibria of a Coupled Ocean-Atmosphere Model. *J. Climate,* **1 (9)**, 841-866.

——, and ——, 1995: Simulation of abrupt climate change induced by freshwater input to the North Atlantic ocean. *Nature*, **378**, 165-167.

——, and ——, 1999: The role of thermohaline circulation in climate. *Tellus,* **51A**, 91-109.

——, and ——, 1999: Are two modes of thermohaline circulation stable? *Tellus,* 51A(3), 400-411.

Mikolajewicz, U and R. Voss, 2000: The role of the individual air-sea flux component in CO2-induced changes of the ocean's circulation and climate. *Climate Dyn.,* **16**, 627-642.

Prange, M., G. Lohmann, and A. Paul, 2003: Influence of vertical mixing on the thermohaline hysteresis: analyses of an OGCM. *J. Phys. Oceanogr.,* **33**, 1707-1721.

Rahmstorf, S., 1995: Bifurcations of the Atlantic thermohaline circulation in response to changes in the hydrological cycle. *Nature,* **378**, 145-149.

——, 1996: On the freshwater forcing and transport of the Atlantic thermohaline circulation. *Climate Dyn.,* **419,** 207-214.

Rind, D., P. deMenocal, G. Russell, S. Sheth, D. Collins, G. Schmidt, and J. Teller, 2001: Effects of glacial meltwater in the GISS coupled atmosphere-ocean model. *J. Geophys. Res.,* **106**, 27335-27353.

Romanova, V., M. Prange and G. Lohmann, 2004: Stability of the glacial thermohaline circulation and its dependence on the background hydrological cycle. *Climate Dyn.,* **22**, 527-538.

Schiller, A., U. Mikolajewicz, and R. Voss, 1997: The Stability of the North Atlantic thermohaline circulation in a coupled ocean-atmosphere general circulation model, *Climate Dyn.,* **13**, 325-347.

Schmidt, M. W., H. J. Spero, and D. W. Lea, 2004: Links between salinity variation in the Caribbean and North Atlantic thermohaline circulation. *Nature*, **428**, 160-163.

Schmittner, A. and A. J. Weaver, 2001: Dependence of multiple climate states on ocean mixing parameters. *Geophys. Res. Lett.*, **28,** 1027-1030.

Schmitz, W. J. Jr., M. S. McCartney, 1993: On the North Atlantic circulation, *Rev. Geophys.*, 31(1), 29-50, 10.1029/92RG02583.

Stocker, T. F. and D. G. Wright, 1991: Rapid transitions of the ocean's deep circulation induced by changes in surface water fluxes. *Nature*, **351**, 729-732.

—— and A. Schmittner, 1997: Influence of CO_2 emission rates on the stability of the thermohaline circulation. *Nature,* **388**, 862-865.

Stommel, H. M., 1961: Thermohaline convection with two stable regimes of flow. *Tellus* **13,** 224-230.

Stouffer, R. J., 2004: Time scales of climate response. *J. Climate*, **17(1)**, 209-217.

Thorpe, R. B., Gregory, J. M., Johns, T. C., Wood, R. A. and Mitchell, J. F. B., 2001: Mechanisms determining the Atlantic thermohaline circulation response to greenhouse gas forcing in a non-flux-adjusted coupled climate model. *J. Climate*, **14**, 3,102-3,116.

Timmermann, A., M. Latif, R. Voss, and A. Groetzner, 1998: Northern hemispheric interdecadal variability: a coupled air-sea mode. *J. Climate*, **11**, 1906-1931.

Vellinga, M., and R. Wood, 2002: Global climatic impacts of a collapse of the Atlantic thermohaline circulation. *Climatic Change,* **54,** 251-267.

——, R. A. Wood, and J. M. Gregory, 2002: Processes governing the recovery of a perturbed thermohaline circulation in HadCM3. *J. Climate,* **15,** 764-780.

Vries, P. de, and S.L. Weber, 2005: The Atlantic freshwater budget as a diagnostic for the existence of a stable shut-down of the meridional overturning circulation, *Geophy. Res. Lett.*, in press.

Weaver, A. J., and E.S. Sarachik, 1991: Evidence for decadal variability in an ocean general circulation model: An advective mechanism. Atmosphere-Ocean, R. W. Stewart Symposium Special Edition, 29, 197-231.

—— and C. Hillaire-Marcel, 2004: Global warming and the next ice age. *Science*, **304**, 400-402.

Wood, R. A, A. B. Keen, J. F. B. Mitchell & J. M. Gregory 1999: Changing spatial structure of the thermohaline circulation in response to atmospheric CO2 forcing in a climate model. *Nature*, **399**, 572-575.

Wunsch, C, 2002: What is the Thermohaline Circulation? *Science*, **298**, 1179.